GBT Memorandum No. 285

Properties of the GBT at L-Band for Commensal Observing

Ronald J Maddalena
August 16, 2013

On the morning of August 4 I tested the L-Band receiver of the GBT at turret rotations other than that at which the receiver is at the focal point of the telescope. These measurements showed an increase in system temperature and a loss in efficiency. Of the eight turret positions, I believe that three (the on-axis and the two adjacent positions) are suited for commensal observations. The next two rotations maybe useful but are somewhat compromised. The remaining three positions have such poor performance that probably no one would want to use them.

Observations and Turret Details

When the rotation is ~360°, (designated N=1 in the antenna manager; see Table 1), the L-band receiver is in the focus rotation. I observed with the receiver at N=1 in order to have a comparison for the performance at other rotations. I then tested the receiver's performance at N=5 and 3. I ran out of time before I could test N=2 or 4. From symmetry, one can expect the performance at N=6 to be similar to N=4; N=7 to be similar to N=3; and N=8 to be similar to N=2. I used the calibrator source 3C48, which has an approximate flux of 14 Jy at 1420 MHz.

The phase center of each feed is ~1.42 m from the axis of rotation of the turret. The ΔX and ΔY columns in Table 1 are the approximate distances in the cross elevation and elevation direction that the L-band feed will be moved from its on-focus location. D is the total distance the feed will be offset. ΔZ and ΔZ/λ approximates the amount by which the feed will be out of focus in m and in units of wavelengths, respectively Using the telescope's plate scale of ~18.1'/m, columns ΔAZ and ΔEL are the expected pointing offset for the given ΔX and ΔY. ΔΘ is the total angular offset at each rotation. The last column give the angular offset in units of the FWHM beam size.

Table 1

N	Approximate Rotation Angle(°)	ΔX(m)	ΔY(m)	D(m)	ΔZ(m)	ΔZ/λ	ΔAZ(')	ΔEL(')	ΔΘ(')	ΔΘ/FWHM
1	360	0	0	0	0	0	0	0	0	0
2	299	-1.24	-0.73	1.44	0.07	0.32	22.5	-13.2	26.1	3.0
3	260	-1.40	-1.67	2.19	0.16	0.75	25.3	-30.2	39.4	4.5
4	219	-0.89	2.52	2.68	0.24	1.12	16.2	-45.7	48.5	5.6
5	180	0	-2.84	2.84	0.26	1.25	0	-51.5	51.5	5.9
6	139	0.93	-2.49	2.66	0.23	1.10	-16.9	-45.2	48.2	5.5
7	99	1.40	-1.64	2.16	0.15	0.73	-25.4	-29.8	39.1	4.5
8	59	1.22	-0.69	1.40	0.06	0.31	-22.1	-12.5	25.4	2.9

The AutoPeak observing directive in the Astrid control system slews the telescopes in orthogonal directions through a source (see the GBT observing manual for details). Before the N=3 and N=5 measurements, I adjusted the pointing of the telescope by the ΔAZ and ΔEL of Table 1 so that the source would be close to the center of the new beam. From the observations, Astrid determines the system temperature, beam width, and the antenna temperature. Figures 1-3 are screen dumps of the Astrid results for the three turret positions. The way in which Astrid updates pointing offsets during an AutoPeak ensures that the telescope moved directly through the source position for the two scans in the last row in the figures. To determine the loss in aperture efficiency at N=3 and 5 one compares the antenna temperatures for the last two scans in each figure for N=3 and 5 to that of N=1. Astrid also provides the results of the pointing fits, which can then be compared to that predicted in Table 1. Table 2 summarizes the measurements.

Figure 1 : N = 1

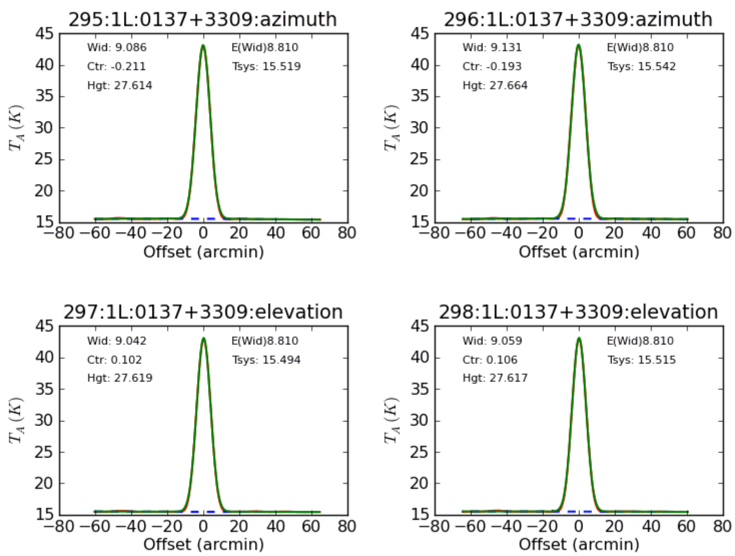

Figure 2: N = 3

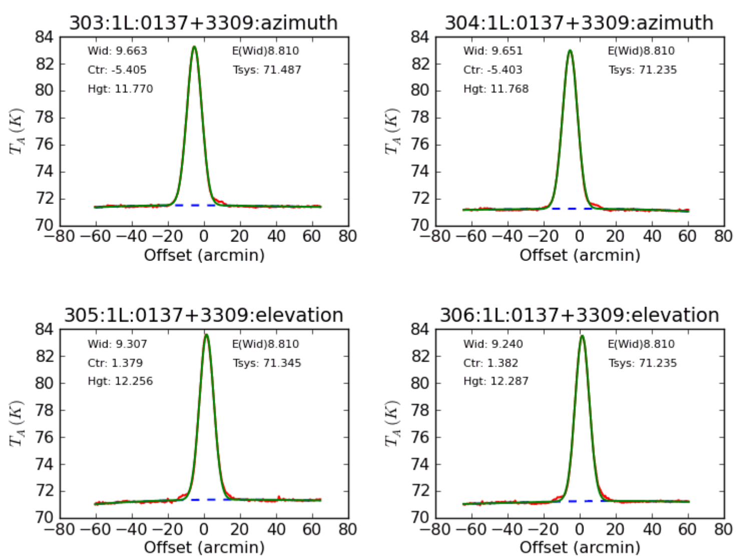

Figure 3 : N = 5

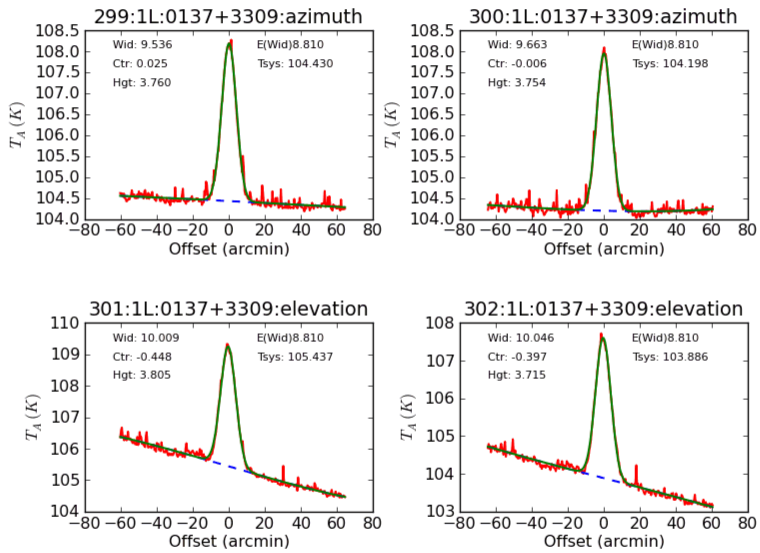

Table 2

N	T_{SYS}(K)	Δ T_{SYS}(K)	T_A(K)	$T_A(N)/T_A(N=1)$	η_A	ΔAZ_{Obs}(')	ΔEL_{Obs}(')	ΔAZ_{Rel}(')	ΔEL_{Rel}(')
1	15.5	--	21.62	--	0.70	-0.20	+0.10	--	--
3	71.3	55.8	12.27	0.568	0.40	24.6	-26.62	24.8	-26.72
5	104.5	89..0	3.76	0.174	0.12	-0.20	-47.53	0.0	-47.63

Analysis

The ΔAZ_{Rel} and ΔEL_{Rel} in Table 2 show the amount by which the pointing would need to be adjusted in any commensal program. Given the crudeness of my optical and geometric modeling, these values agree with my first-cut predictions from Table 1. In contrast, the most striking feature in Table 2 is the increase in T_{SYS} and decrease in aperture efficiency, η_A, when the receiver is at positions other than N=1.

It is very doubtful that the loss in efficiency is related to optical aberrations from coma or from axial defocusing. From eq. 14 of Ruze (*IEEE Trans. Antenna & Prop*, **AP-13**, p. 660, 1965), within an angular diameter of ~80 FWHM there should be at most a 1 dB loss due to coma for the GBT's f/D = 1.9 at Cassegrain focus. The $\Delta\Theta$/FWHM column of Table 1 shows we never approach this. Using the approximations for $\Delta Z(m)/\lambda$ in Table 1 and §III.B of Baars (*IEEE Trans. Antenna & Prop*, Vol **AP-21**, p. 461, 1973), the loss in gain due to axial focusing should be well under 1% for N=5 and 3.

I've always worried whether losses due to structural obstructions or vignetting would be important. On August 6, I took photographs from the top of various turret positions toward the subreflector to determine structural obstructions (Figures 4-9). At the time it was not possible to rotate the turret and, thus, I couldn't exactly place the camera at all turret location at the expected location of the L-band's phase center. Instead, I sometimes had to place the camera on top of the receiver that was located at a turret position. The perspective for locations N=1, 6, 8, and 9 is close to being perfect as these locations either had covering plates (instead of a receiver) or a receiver with a relatively short feed. At N=3 and 7, the respective locations of the L- and S-band receivers, the perspective in these photos are from a higher location then the phase center due to the substantial height of these receiver's feeds. The N=7 photograph is a truer representation then N=3 since S-band's feed is shorter than the L-

Figure 4: N = 1

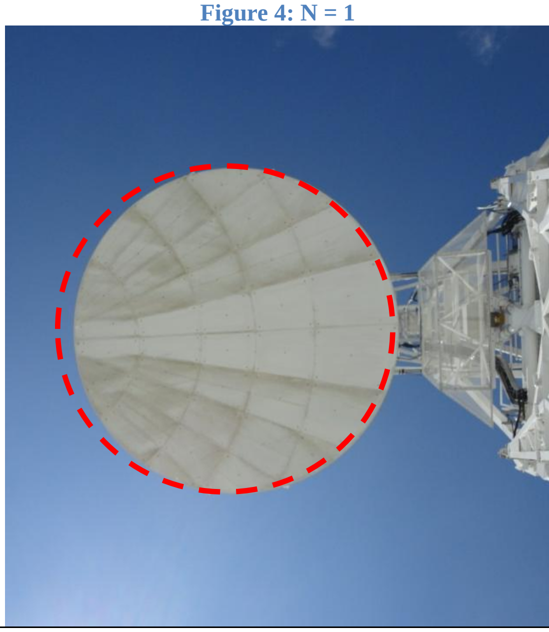

Figure 5: N=8

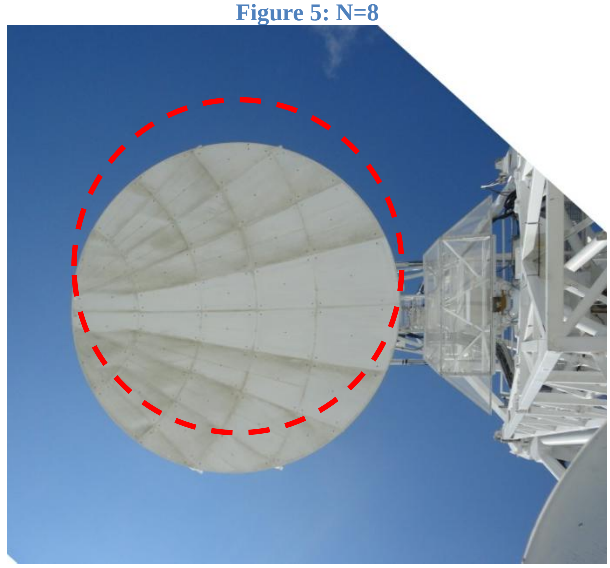

Figure 6: N=3

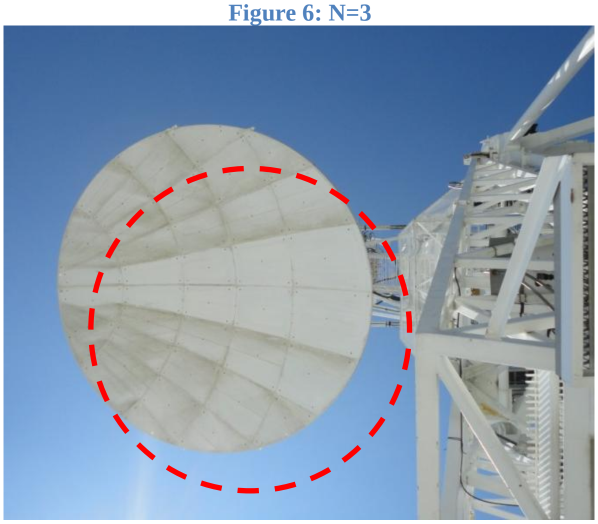

Figure 7: N=7

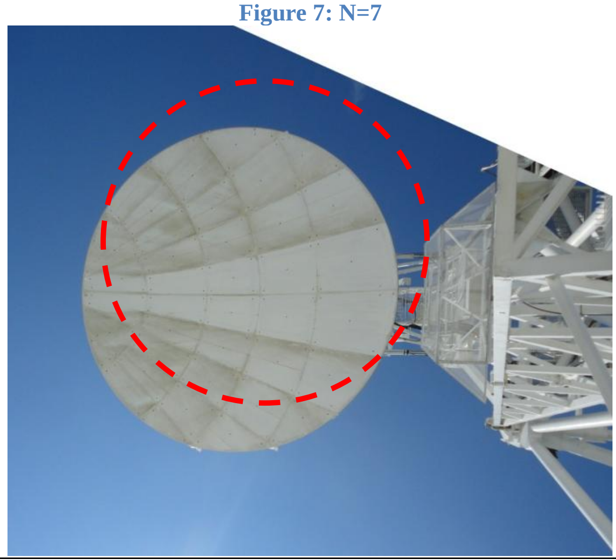

Figure 8: N=5

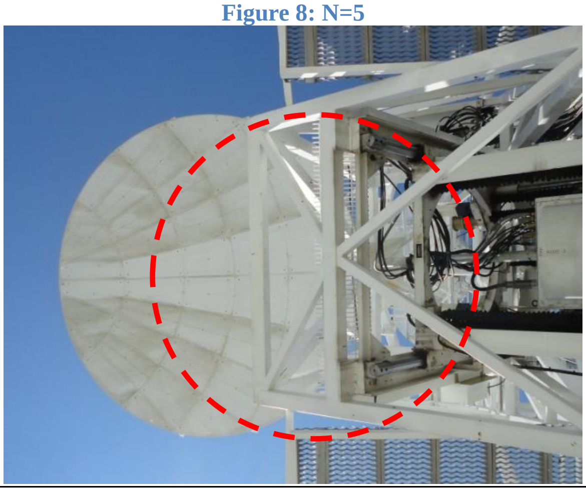

Figure 9: N=6

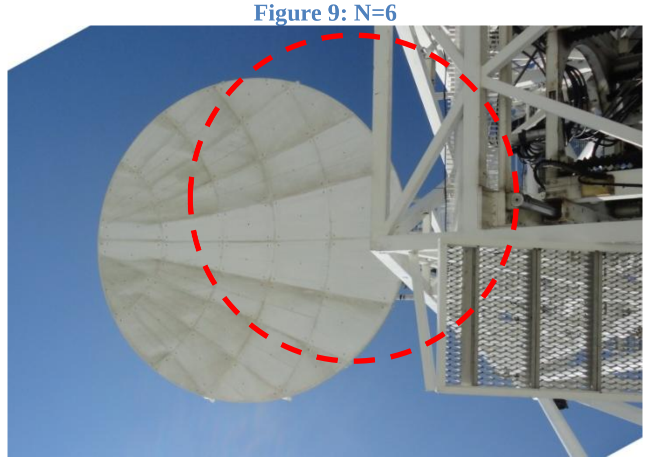

band feed. Due to the symmetry of turret locations, there was no need to take photographs from N=2 and 4. The red circles drawn over the photographs roughly illustrate the -13 dB limit in the feed illumination pattern.

Clearly we have substantial obstructions for N=5, 6, and, by inference, 4 from the retracted prime focus boom. The obstruction may be the cause of the low efficiency for the N=5 observations and might contribute to the high T_{SYS} at N=5. It is unlikely that N=3 and 7 has substantial loss in efficiency due to obstructions. Since any obstruction at N=3 and 7 appears to be falling on the spillover shields, which are directed toward the sky, the obstruction for these locations are probably not the cause of any substantial increase in T_{SYS}. N=2 and 8 seem to be as unobstructed as N=1.

Until I saw the results of the measurements, I thought vignetting would only arise as the center of the feed's illumination shifted away from the center of the subreflector for all but the N=1 position, as the red outlines in Figures 4-9 show. The efficiency will drop as the value of D in Table 1 increases because the center of the feed's illumination moves more and more toward the subreflector's edge, as depicted in the photographs. Since feed illumination patterns don't have sharp edges but are approximate Gaussians, as some of the Gaussian illumination moves off one side of the subreflector onto cold sky, it is partly compensated by the illumination on the opposite side of the subreflector that was on the sky but is now moved onto the subreflector. Thus, the actual loss in efficiency should be less than the percentage of the subreflector area that seems to be unused in the photographs.

I also expected we would not see an increase in T_{SYS} since the vignetting depicted in the photographs falls onto cold sky for those turret locations that have no structural obstructions. However, I had not realized there was a second cause of vignetting that would produce more loss in efficiency and that would also result in higher T_{SYS}.

The second cause for the loss in efficiency from vignetting arises from some part of the illumination from the subreflector missing the main dish completely. Since the illumination that misses the dish falls onto the ground, the rear-spillover increases which, in turn, produces an increase in T_{SYS}.

Figure 10 is a not-to-scale sketch of the GBT optics in the cross elevation direction and shows the ray tracings for a feed that is offset the full diameter of the subreflector. Any ray hitting the main dish to the left of 'A' will not enter the receiver since the subreflector ends at point 'a'. Any ray that hits the subreflector between 'e' and 'd' comes from the ground (to the right of 'D') thereby lowering the efficiency as well as increasing T_{SYS}. Any ray that would come to the right of 'e' or to the left of 'a' comes from the forward spillover onto the cold sky. These rays will not increase T_{SYS} but do decrease the efficiency since the feed illumination is centered on 'e' instead of the symmetry point, 'c'.

In the elevation direction, one can use the same figure by imagining that (1) the 'a' – 'c' section of the subreflector does not exist and (2) the main dish does not exist to the left of 'B'. Then, only 'C'-'D' of the main dish will be used and, as before, the 'd'-'e' section of the secondary will receive rays from the ground. Note: since the figure is not to scale, the location of the focal points, f_1 and f_2, and, therefore, the ray tracings are not equivalent for the cross elevation and elevation views. Thus, the percentage useful area of the main dish and subreflector one visualizes from the figure is very misleading. Instead, we would need to use a 3-d ray-tracing program or, better yet, use empirical measurements to determine performance at the turret locations other than the ones measured here.

The beam shape of a telescope is the Fourier Transform of the illumination pattern. Unfortunately, the second cause of vignetting is essentially a bite being taken out of the normally-circular illumination pattern. Thus the beam shape of the telescope will be increasingly compromised as the size of the bite, which is related to the magnitude of D, increases. Figure 2 appears to show an increase in the wings of the beam shape, relative to the on-axis beam in Figure 1.

Figure 10: Sketch of optics for an offset feed

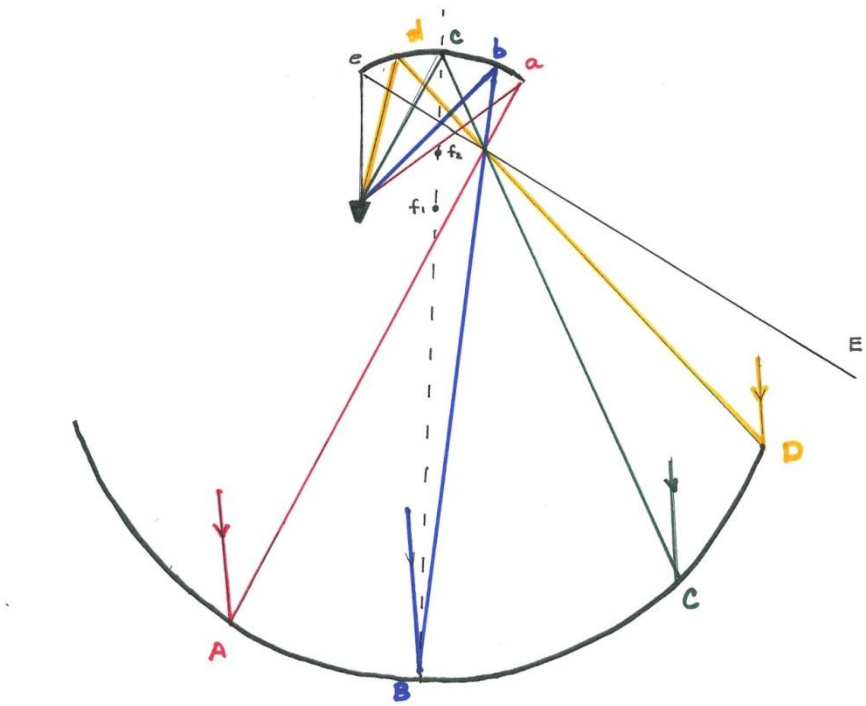

Figure 11: Rough Modeling of Loss in Performance

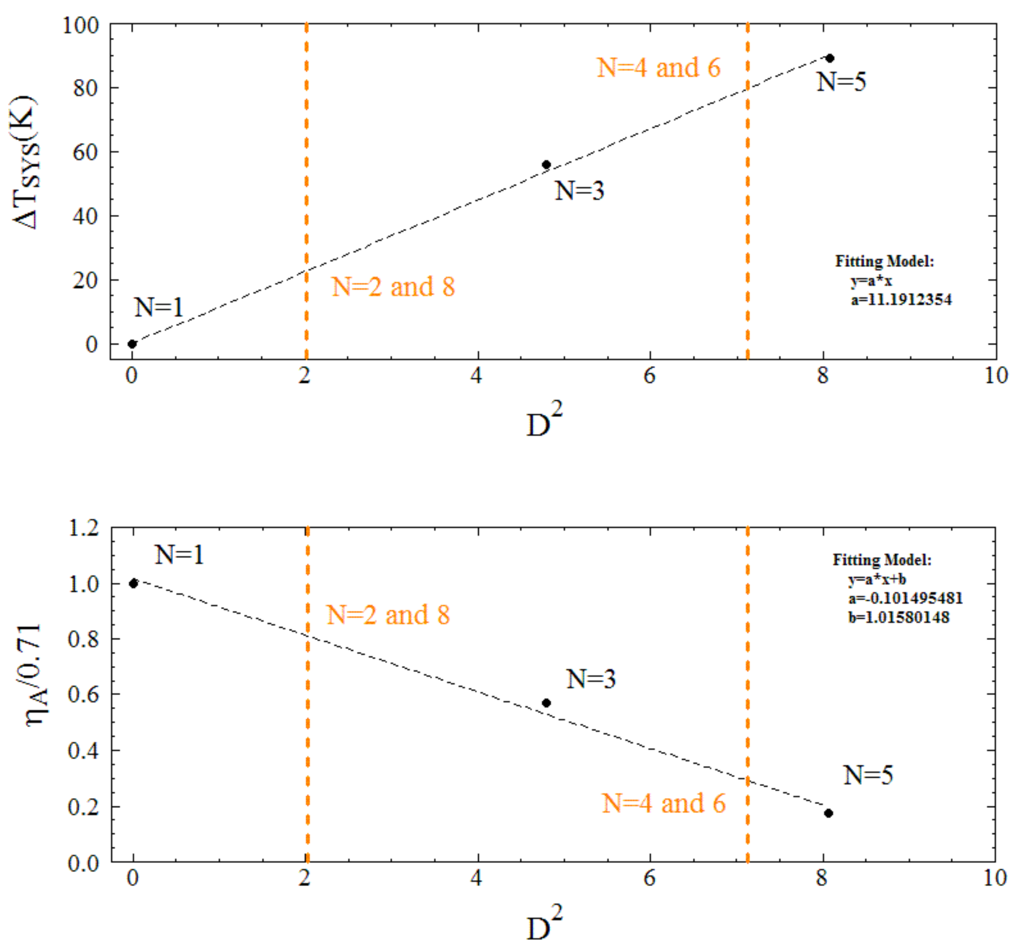

At this point, I think it is important to have some idea of the expected performance, at least for planning, for the N=2 and 8 positions as these are expected to have the best performance after N=1. Figure 11 shows a fit of η_A and ΔT_{SYS} for the N=1, 3, and 5 data (black points) versus D^2 from Table 1. I used a quadratic model mostly from dimensional consideration since η_A and excess ΔT_{SYS} are related to area, which is probably loosely related to D^2. The Figure suggests we might measure $\eta_A \sim 0.56$ and $\Delta T_{SYS} \sim 23$ K for both N=2 and 8.

Thoughts and Conclusion

The measured pointing offsets for N=3 and 5 match well enough to those derived from simple geometry. Measuring the offsets for any of the remaining turret locations should be simple.

The increase in T_{SYS} for N=3 is probably due to a substantial increase in the rear spillover, as sketched in Figure 10. The increase in rear spillover plus the offset in illumination, as depicted in Figures 6 and 7 are the causes of the loss in efficiency for N=3. N=3 and its symmetric location N=7 may be suitable for some projects even with the measured compromise in performance.

We can expect the beam shapes to be increasingly compromised since the size of the 'bite' into the illumination pattern grows as one rotates the turret away from N=1.

Due to the large feed offset for we expect that the performance at N=4, 5, and 6 will be worse than for N=3. N=4, 5, and 6 also have substantial obstructions in their optical path, probably making them less useful then we had hoped.

Although I have not measured the performance at N=2 and 8, the expected telescope performance should be substantially better than that measured at N=3. The feed offsets for these locations are less than N=3, which implies that ΔT_{SYS} should be substantially lower and η_A closer to that when the receiver is in the focus position. Rough modeling suggests $\eta_A \sim 0.56$ and $\Delta T_{SYS} \sim 23$ K for both N=2 and 8. Future empirical measurements are probably easier and more definitive than would be modeling the expected loss in performance.

The one idea I have for improving the performance for N=2, 3, 7, and 8 would entail reducing ΔT_{SYS} by constructing a (costly) ground screen, either on the ground, or around the primary's edge.

Currently the holographic and Mustang receivers are at N=2 and 8, the locations that have the best performance next to N=1. These receivers are used infrequently. Instead, we probably would like at N=2 and 8 receivers that are used frequently, thereby adding more hours when commensal observing will be most profitable. Since the N=2 and 8 have holes that can accommodate any receiver but S-band and L-band itself, it is likely that, with enough persuasion, the receivers can be rearranged in the turret for better commensal observing.

The increase in rear spillover may be linked to an unexpected elevation-dependence of spillover that I and M. E. Mattox measured (http://adsabs.harvard.edu/abs/2012AAS...21942238M and http://www.gb.nrao.edu/~rmaddale/Research/SpilloverAASJan2012d.pdf. Maybe the focus tracking curve, which moves the subreflector as a function of elevation by as much as 0.15 m, produces an optical offset like that sketched in Figure 10. Our results suggest there is a 1 K excess in T_{SYS} at some elevations, which is fair part of the current 16 K at the zenith. Note that the current focus-tracking curve improves performance at high frequencies, where a 1 K increase in T_{SYS} is unimportant. Thus, it might be possible to derive an alternative focus tracking curve that minimizes T_{SYS} which could decrease the noise in observations at L-band by maybe 6%, equivalent to a savings of 12% in observing time.